Metallurgical Factors Affecting Microbial Colonisation and Corrosion of Drinking Water Network Materials

[1]Blanca M. Rosales, [1]Silvia E. Rastelli, [2]Ernesto G. Maffía
[1]CIDEPINT (CIC- CONICET- CCT La Plata)
Av. 52 s/n e/121 y 122, (B1900AYB) La Plata, Argentina

[2]Depto. Mecánica, Fac. Ing. UNLP,
Calles 4 y 116, (B1900AYB) La Plata, Argentina

ABSTRACT

The present work reports the studies performed to investigate the influence of some metallurgical factors in the microbial colonisation and corrosion of drinking water network materials. Cold rolling process applied to row materials submitted to drinking water dynamic tests seems not to affect substrata areas colonisation distribution as compared to as received condition of tubing materials. However, samples exposed to hydrodynamic and static tests with three different accumulated plastic deformation show diverse magnitude of localised attack but non-correlative with the substrata surface energy.

INTRODUCTION

The microbiologic influenced corrosion (MIC) study of drinking water network materials present special interest due to serious potential health problems by pathogenic microbial species, the high costs of maintenance and repairing involved as well as the new material development for this essential infrastructure. The most frequent failures observed in networks after 50 years service are the lack of appropriate water service provision to population. Main causes are blocking of tubing up to stop water circulation and pitting of the underground network.

Characteristic microbial development occurs from the inside of the tubing: *biofilm*. A biofilm is a microbial community characterized by cells attached to a substratum or interface embedded in a matrix of extracellular polymeric substance (EPS) [1,2], where also pathogenic strains could grow and spread by the supposed drinking water [3]. Biological sludge deposited mainly consist of bacteria developed using organic and inorganic nutrient substances stemmed from the diverse water used, mainly from rivers or underground sources. Presence of biological cells and available organic and inorganic nutrients cause the mentioned problems as tubing clogging and MIC up to localised perforation after long time service.

Concerning the latter, several forms of corrosion have been reported, although pitting starting in blowings in the cast iron tubing of old technologies was the most frequently found cause of perforation when analysed the Buenos Aires city network [4]. Another attack observed in almost all studied sections was graphitization caused by iron selective dissolution without any change in the net wall thickness under biofilm deposits.

Besides, in previous research work about MIC it was shown that certain metallurgical factors affected corrosion of diverse metals and alloys [5], more intensely than in the low aggressiveness environment of drinking water.

The main purpose of this work is to reveal the rolling effect introduced to avoid water laminar flux alteration during hydrodynamic test of thick row material samples. It was considered of interest to evaluate metallurgical factors not previously considered in order to shed light on the relative incidence on the soft MIC attack observed in service conditions and during this project [4,6,7].

EXPERIMENTAL

Test samples of low C steel (instead of cast iron), pure Zn (Zn 98%; Cu 1%; Ti + Mg 1%) to simulate the galvanized steel surface, hidrobronze and polypropylene (PP) were prepared in three surface energy conditions and two thickness. Polypropylene (PP) is a propylene-ethylene random copolymer as determined with a FTIR Nicolet 5700- Omnic and a Mettler DSC-822. The latter characterization was performed between 25 °C to 200 °C at a heating rate of 10 °C/min, under N_2 atmosphere showing a melting point of 142 °C. Samples were used in 4 replicates cut to 10 x 10 mm on (a) their original **Fe** thickness, of 0.7 mm (NL), (b) after 250% cold rolling up to 200 µm (L) and (c) same as (a) with further annealing during 1 h at 538ºC (LR). Three replicate samples were grinded up to 600 grade emery paper for microbial counting and one was polished up to 0.25 µm surface finishing for ESEM characterization after the 25-day circulation test.

All of them were degreased with acetone and rinsed with distilled water. Back faces of the 4 replicates, in the 3 energy conditions of all materials were masked with a silicone base adhesive and then fixed to a polyethylene support.

Installed inside acrylic cylindrical cells in a sterile chamber two laboratory circuits were fed with drinking water of La Plata city stored in two 50 l covered plastic tanks. One of the tanks contained the same drinking water, additioned with analytical grade reagent $Na_2HAsO_4.7H_2O$ in a 5,000 As^{+5} µg.l $^{-1}$, to determine the effect of microbial population resistant to As and the one grown in its absence, as in previous papers [3,4].

“Aged” solutions were employed for these test Series to know the initial bacterial community inoculums of both water compositions. On the contrary when fresh tap water was charged on each tank initial total counting could not be determined by culture up to complete Cl_2 evaporation respect to the beginning of the hydrodynamic tests due to the free chlorine stress effect on bacterial survival (3-4 days). It takes 24 to 48 h after Cl_2 finish to evaporate, but only at the third to fourth day total microbial counting becomes positive.

Microbial Characterization

At the end of the circulation test the harvested deposit from all materials was softly scraped from each sample with a sterile spatula on triplicate in 1ml of sterile physiologic solution. Once dilution to 1/10 was performed, 100 µl was seeded in nutrient agar medium (plurypeptone 5.00 g.l $^{-1}$, beef extract 3.00 g.l $^{-1}$, sodium chloride 8.00 g.l $^{-1}$, agar 15.00 g.l $^{-1}$) and incubated 48 hs at 25 ºC, for further counting.

Surface analysis of Fe

Metallurgical surface characterization was performed on all non-exposed **Fe** samples to reveal the initial surface structure and further alteration during rolling and annealing. Metallographic structure development was performed with Nital 2 (2% HNO_3 in ethylic alcohol) on 0.25 µm diamond paste surface finishing of the respective **Fe** samples.

A scanning electron microscopy (ESEM) FEI Quanta 200 was used for surface morphology characterization as well as for analysis of the accumulated products on samples. Deposits removal from the single polished **Fe** sample of each surface energy condition was performed by picking in HCl 50% solution additioned to 3 % with urotropine as **Fe** inhibitor. ESEM analysis was performed on the underlying attack.

Short duration tests

1.- Due to the intense degradation observed on samples after 25 days of exposure to both circuits in the absence and presence of As short duration tests were performed during 3 days and 1 day on polished **Fe** samples in the three surface energy conditions (LR, L, NL) for SEM characterisation.

2.- Also with the same surface finishing, **Fe** samples were exposed to sterile, static drinking water with and without As in the 3 surface energy conditions to determine the attack morphology produced during 3 days .
3.- Idem 2, exposed to drinking water from both circuits.
4.- Drop test on **Fe** in sterile condition was performed in a laminar flux chamber on **Fe** grinded to 1500 emery paper in 2 surface energy conditions L and NL . Each sample was inoculated with a small piece of two strains of the microbial species harvested on **Fe** samples after the 25-day test from both circuits. The 2 bacterial isolates seeded from the circuit in the absence of As were a salmon and a white coloured colonies as well as from the tank in the presence of As.

X-ray diffraction on products deposited on all materials
Three replicate samples of 10 x 100 mm were submitted to a separate circulation test Series of the 4 materials, during 15 days, to have enough corrosion products for X-ray diffraction characterization. The equipment used was a Philips 3020 with PW 3710, Cu-Kα radiation, Ni filter 40 kV-20 mA, without monochromator in the 2θ scanning range 5º - 70º.

RESULTS

Analogous random distribution of corrosion products was observed at the naked eye on all the tested materials. The same uneven colonisation aspect was maintained amongst all replicate samples to those shown in previous papers on cold rolled samples [6,7].

Microbial Characterization
Microbial counting of the harvested deposits on all materials for the different surface conditions are shown in Table 1. The final total counting presented the same high dispersion previously observed in the presence and in the absence of As [6,7].

Surface analysis of Fe
The observed metalographies were coincident with structures produced by sterile drinking water in the 3 surfaces energy conditions.

Short duration tests
1.- Corrosion attacks produced on the 3 different energy conditions of **Fe** are shown in Fig. 1 a) to d) after 3-day test in both circuits. However, the 2 different attack morphologies detected when samples were exposed to both circuits in the presence of microbial species seemed to be caused by bacterial strains grown according to selection caused by the As^{+5} tolerance. Even when 3 days produced quite incipient surface area percentage attack on each of the **Fe** surface condition diverse stages of the 2 alternative microbial corrosion processes were noticed. On different regions of the same sample for each surface energy condition, certain areas revealed preferential hemispherical with polished bottom pitting of similar size or smaller crystallographic pits revealing the typical **Fe** structure. Those very different morphologies were correlated with MIC produced by strains grown in the different circuits.
Most densely spread attack showed generally bigger corrosion structures than areas with the same morphology but small size, revealing a further attack stage by the same corrosive microbial strain depending on the circuit.
The ESEM shortest test results, after 1-day circulation, are shown in Fig. 2 a) to c). In the most incipient attack performed during hydrodynamic test for “1 day circulation” in both circuits ESEM analysis also revealed the attack morphology experienced by the **Fe** surface polished up to 0.25 μm. The Beilby thin film formed during this mechanical cold

work uniformly affected all the polished sample surfaces not interfering with the blistering also observed in other types of corrosion during **Fe** attack nucleation [5]. These alterations were best observed during this short duration tests in both circuits due to the minimum incidence of microbial species effect.
A generalised blistering appeared on the whole surface caused by underlying corrosion products of Fe below the disturbed film once immersion started, as can be seen in Fig. 2. The structure development by grain boundary attack was evident in some micrographs below the Beilby layer and on areas where it was fractured or missing. This allowed verification of the LR equiaxial grains in the presence of As (Fig. 2 a) and NL as received samples, in the absence of As (Fig. 2 c). For the L surface condition a panoramic view (x 500) shows an apparent rolling effect on the morphology and localised circular attack nucleation around anodic and cathodic inclusions respect to the Fe matrix (Fig.2 b).
2.- Static 3-day duration test in sterile drinking water in the absence and in the presence of As was also performed on polished samples. ESEM analyses allowed identification of the **Fe** structure development produced by sterile drinking water (Fig. 3).
The macroscopic aspect of the attack allowed connecting the preferred colonization areas to a more intense corrosion effect by the biofilm settlement where dense pitting nucleated. However, a big proportion of non-damaged surface was found on all the analysed conditions with very limited isolate attacks.
3.- The ESEM aspect of the attacks nucleated on **Fe** during the 3-day immersion in static drinking water from both circuits revealed the same microbial attacks (Fig. 4 a) to c). Faster nucleation was found in As containing drinking water than in its absence and a rough texture around localised pitting.
4.- The culture of the strains isolated from both circuits detailed in Table 1 showed differences in colour, size and textures, which allowed a qualitative correlation amongst the naked eye colour and both ESEM bacterial aspect and attack morphologies. Comparison of the ESEM micrographs allowed correlating the aspect of bacteria from the seeded strains with their attack morphology, as can be seen in Fig. 5.
Fig. 5 a) shows different details of the bacillus (salmon strain), with underlying crystallographic attack (absence of As) and Fig. 5 b), c) white and salmon strains aspect causing hemispherical attacks (presence of As).
The corrosion nucleation on **Fe** show surface blistering on both polished and grinded samples finishing, below the 4 microbial strains harvested on **Fe** from both circuits. Associated to the surface condition Fig 5a) shows long grains and Fig 5 d) reveals equiaxial grains. Various SEM view showed the presence of bacillus in the biofilms and the cross section aspect of **Fe** blistering revealing crystallographic attack along the whole thickness of metal blisters.

X-ray diffraction on products deposited on all materials

The products detected on each material are shown in Table 2.

DISCUSSION

Based on the results displayed it may be noticed that the uneven substratum colonization is independent on the material and surface energy condition for all the materials tested.
The different susceptibility found amongst all the materials seems to be mainly controlled by the microbial species growing in the presence or in the absence of As than by the surface energy of the tested **Fe** samples. Colonisation results were not modified respect to those observed in previous works [6,7].
The corrosion attack nucleation, on the contrary revealed correlation with the microbial growth of different strains more than to the processes applied to modify the surface energy of the **Fe** samples analysed. For very initial corrosion steps crystallographic pitting was

observed on the 3 surface energy conditions on **Fe** in the absence of As while hemispherical attack with polished bottom was found in the presence of As (Fig. 2). Polished bottoms consisted on corrosion products which in some areas appeared broken, partially missing or completely disappeared according to the various stages observed for each type of attack. All these aspects were also found during drop tests on the **Fe** abraded samples including structure development in the absence and presence of As.
Surface roughness or irregularities as scratches or even grain boundaries did not evidence any effect on biofilm settlement, attachment and attack nucleation. Moreover, sterile static drinking water both in the presence and in the absence of As seemed to produce the same uneven distribution.
Neither colonisation nor corrosion nucleation showed evidence of any attachment difficulty on polished surfaces to 0.25 μm respect to **Fe** surface grinded to 1500 paper.
For the three surface energy conditions all metals evidenced the same uneven colonization as that found at the naked eye amongst all replicates.
Biofilm adherence controlled localised underlying attack distribution.

CONCLUSIONS

EPS and corrosion products random distribution on metal samples was independent of the surface energy condition.
Depending on the absence and presence of As in the drinking water, 2 different attack morphologies were found.
Corrosion nucleation of the localized metallic attack depended more on the presence or absence of As than from the surface energy condition during the hydrodynamic and static tests.
The presence of As resulted in higher drinking water aggressiveness only by stimulation of the most tolerant to As^{+5} and corrosive microbial species growth.
Corrosion nucleation on **Fe** below 4 microbial strains harvested from both circuits produced surface blistering on polished and on grinded sample finishing.
Surface roughness did neither affect biofilm attachment nor underlying MIC.
Sterile drinking water only produced **Fe** structure development in the presence and in the absence of As, both during static and dynamic tests.
ESEM analysis showed correlation amongst bacterial species and **Fe** attack morphology in hydrodynamic and static tests exposed to drinking water from both circuits.

Material	**L R**		**L**		**NL**	
	without As	with As	without As	with As	without As	with As
Fe	$1,5 \times 10^4$	1×10^5	4×10^4	7×10^4	2×10^5	7×10^5
Zn	$2,5 \times 10^4$	1×10^5	$2,5 \times 10^4$	1×10^5	$7,5 \times 10^3$	$7,5 \times 10^4$
Cu	$8,5 \times 10^2$	4×10^3	$8,5 \times 10^2$	1×10^3	$3,5 \times 10^2$	1×10^3
PP	2×10^3	$6,5 \times 10^3$	1×10^3	1×10^4	1×10^3	1×10^4

Table 1. Total microbial counting ($UFC.ml^{-1}$) on all tested materials in the absence and presence of As after 25-day circulation test.

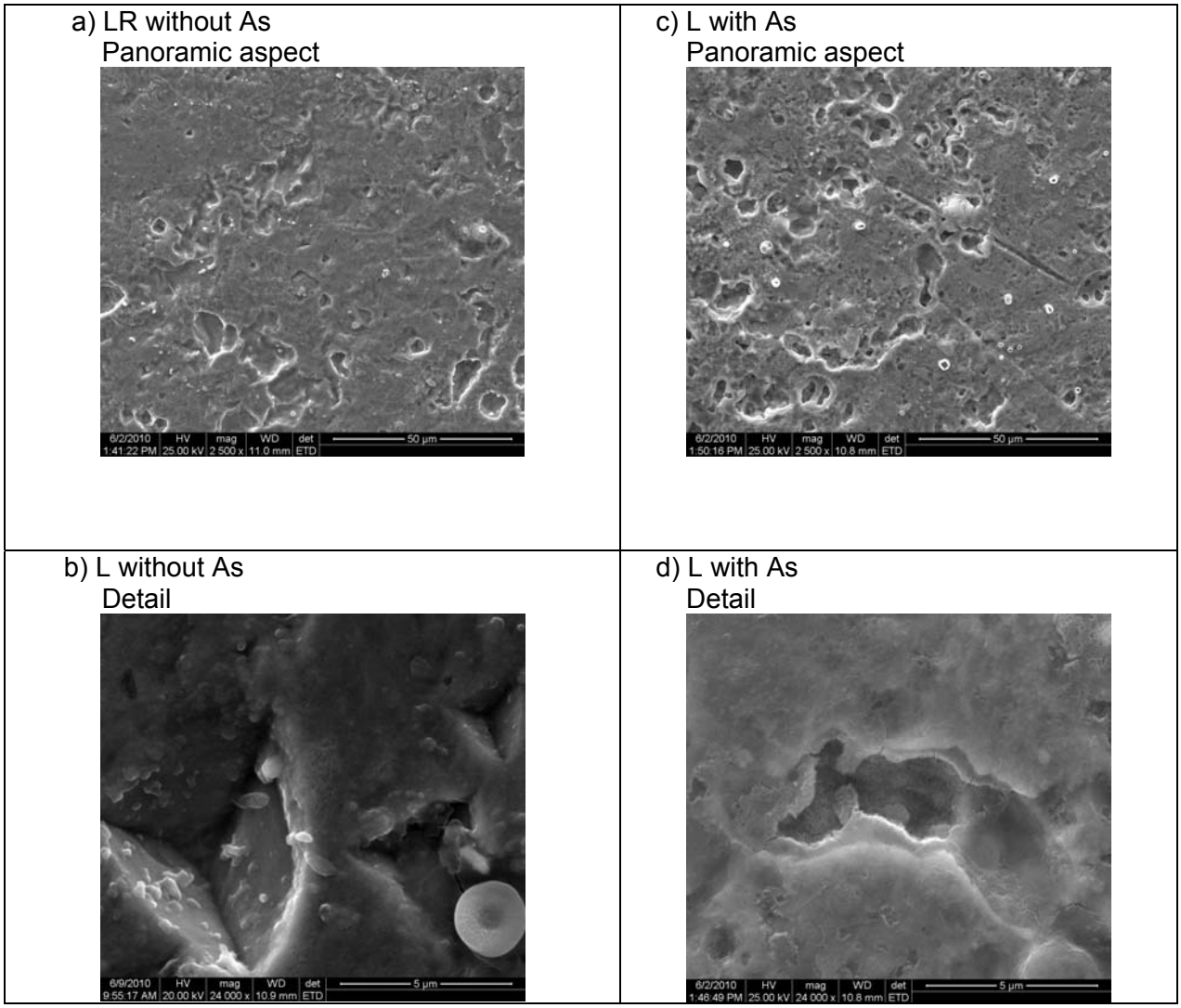

Figure 1. ESEM aspect of **Fe** polished samples to 0.25 μm in different surface energy conditions: a) LR without As, b) L without As, c) L with As, after 3-day circulation test.

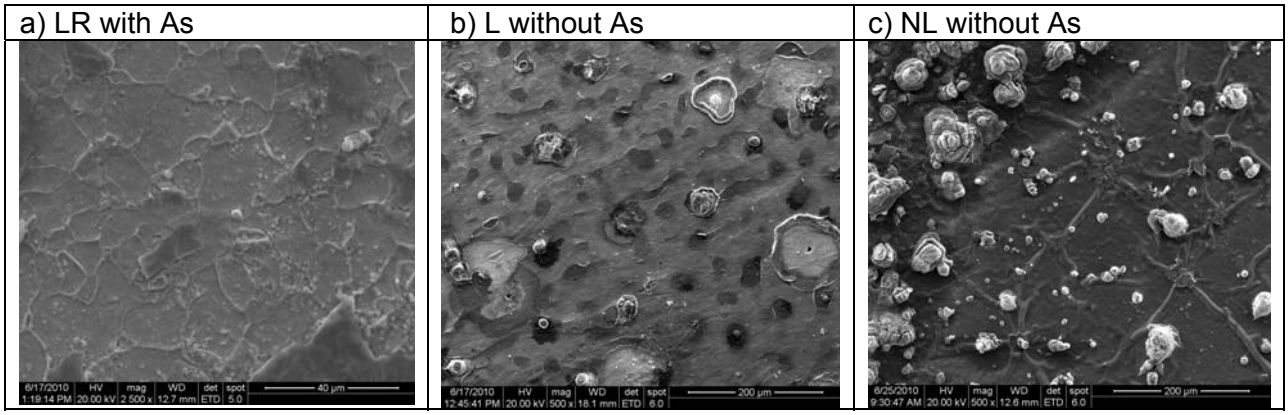

Figure 2. ESEM aspect of **Fe** polished samples to 0.25 μm in 3 different surface energy conditions after 1-day circulation test.

a) LR with As	b) L with As	c) NL without As
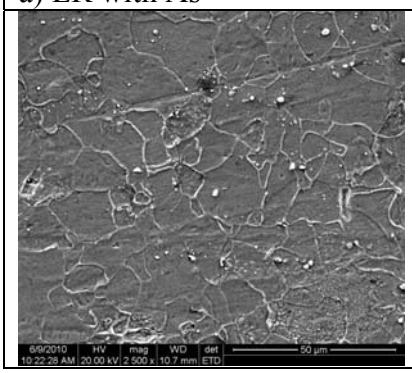	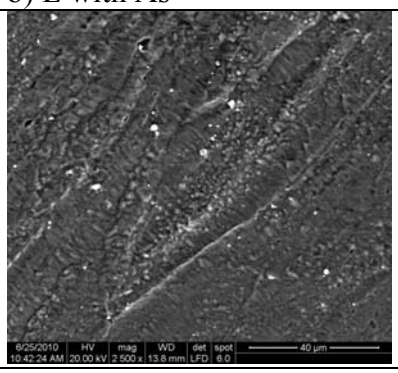	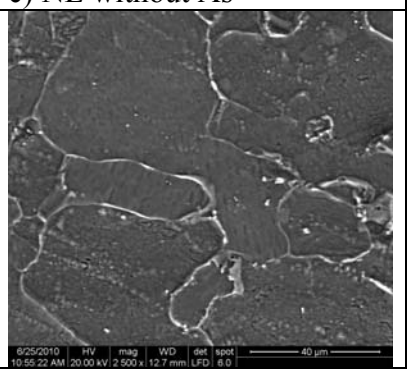

Figure 3. ESEM aspect of **Fe** polished samples to 0.25 µm in 3 different surface energy conditions after 3-day sterile static test.

a) LR without As	b) L without As	c) NL with As
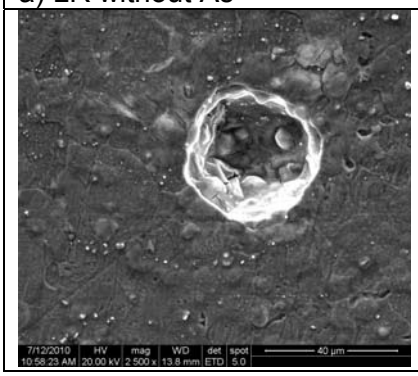	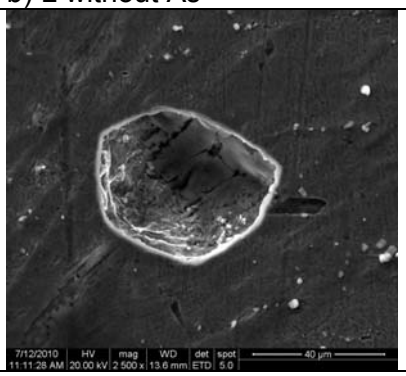	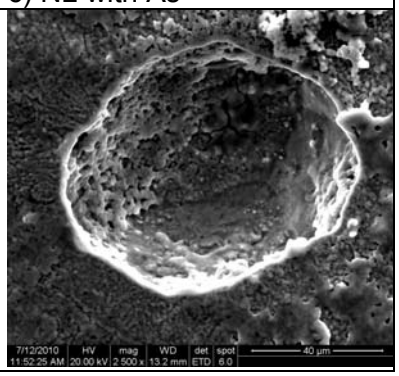

Figure 4. ESEM aspect of **Fe** polished samples to 0.25 µm in the 3 surface energy conditions: a) LR, b) L and c) NL after 3-day static immersion in drinking water from both circuits.

a) Salmon strain from circuit without As, on L sample	c) White strain from circuit with As, on L sample
	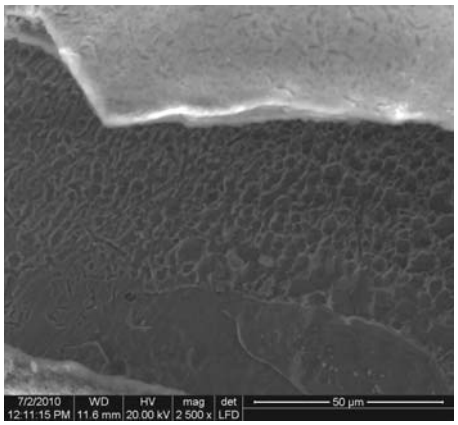

b) idem a): detail

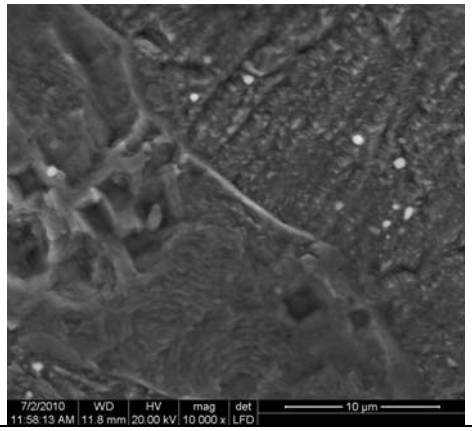

d) Salmon strain from circuit with As, on NL sample

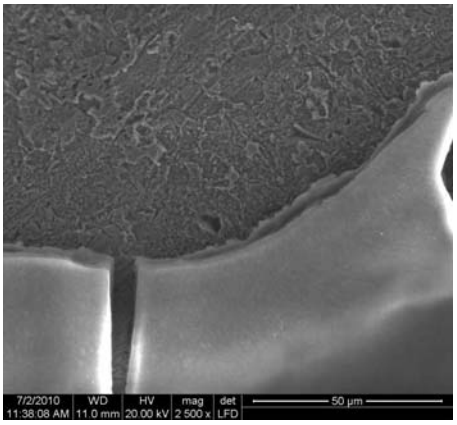

Figure 5. ESEM aspect of **Fe** grinded to 1500 samples in the 3 surface energy conditions: a)-b) LR, c) L and d) NL, after drop test below bacterial strains from each of both circuits.

Material	**Products Found on samples exposed to both circuits**
Fe	Abundant amorphous material; 2 picks at 3.26-3.02 degree
Zn	Metallic base (Znº);Zn basic carbonate and chloride: $Zn_5(CO_3)_2(OH)_6$ (hidrozincite); $Zn_5(OH)_8Cl_2.H_2O$ Zinc-metaarsenite $Zn(AsO_2)_2$
Hidrobronze	Metallic base (Cuº); Cuprite (Cu_2O)
PP	Organic phase polypropylene $(C_3H_6)_n$; Claudetite (As_2O_3)

Table 2. X-Ray diffraction results obtained from deposits on all the tested materials.

REFERENCES

[1] M.E. Shirtliff, J.T. Mader, A.K. Camper. “Molecular Interactions in Biofilms” Chemistry & Biology, Vol.9, p. 859 (2002).

[2] I. B. Beech, J.A.Sunner, Hiraoka K. “Microbe-surface interactions in biofouling an biocorrosion processes” International Microbiology Vol. 8 p.157(2005).

[3] F. Teng, Y.T. Guan, W.P. Zhu. Effect of biofilm on cast iron pipe corrosion in drinking water distribution system: Corrosion scales characterization and microbial community structure investigation. Corrosion Science Vol.50 p.2816 (2008)

[4] B. Rosales. “Residual useful life estimate of the Buenos Aires drinking water network”. Ed. O.E. Scarpati and J.A. Jones, Orientación Gráfica, ISBN 978-987-9260-46-3 (2007).

[5] B.M. Rosales and M. Iannuzzi. “Aluminium AA 2024T351 aeronautical alloy- Part 1 Microbial Influenced Corrosion analysis”. Materials Science and Engineering A, Elsevier, Materials Engineering A, 472, (1-2), 15-25, ISSN 0921-5093 (2008).

[6] B. Rosales, M. Pujol and E. Rastelli. “Iinicial steps on microbial colonization and corrosion on drinking water networks”. Proc. XVII Int. Corr. Congress, Las Vegas (2008).

[7] Rastelli S. E., Rosales B., Elsner C. and Pujol E.M. “Microbial biofilm interactions with drinking water network materials”. 7 LABS, Quito, Ecuador, Plenary Lecture. (2009).

[8] B.M Rosales and E.S. Ayllón “Atmospheric marine corrosion of structural steels”. Atmospheric Corrosion, Ed. W. Ailor, John Wiley & Sons, Inc., Chapter 29, p. 423 (1982).